IEEE Access
Multidisciplinary | Rapid Review | Open Access Journal

Received January 3, 2020, accepted January 16, 2020, date of publication January 24, 2020, date of current version January 31, 2020.

Digital Object Identifier 10.1109/ACCESS.2020.2969221

A New Method for Predicting Crosstalk of Random Cable Bundle Based on BAS-BP Neural Network Algorithm

CHAO HUANG[1], YANG ZHAO[1], WEI YAN[1,2], QIANGQIANG LIU[1], AND JIANMING ZHOU[1]

[1]School of Electrical and Automation Engineering, Nanjing Normal University, Nanjing 210046, China
[2]Zhenjiang Institute for Innovation and Development, Nanjing Normal University, Zhenjiang 212004, China

Corresponding author: Wei Yan (61197@njnu.edu.cn)

This work was supported in part by the National Natural Science Foundation of China under Grant 51475246, in part by the National Natural Science Foundation of Jiangsu Province under Grant BK20161019, in part by the Aviation Science Foundation under Grant 20172552017, in part by the Key Project of Social Development in Jiangsu Province under Grant BE2019716, and in part by the Nanjing International Industrial Technology Research and Development Cooperation Project under Grant 201911021.

ABSTRACT Accurate analytical solution for the crosstalk of random cable bundle is difficult to obtain, but the limit of the crosstalk can be predicted. This paper proposes a method to predict the crosstalk of random cable bundle. Based on the idea of cascade method, the model takes into account the random rotation of the cross-section and the random transposition of the core. A neural network algorithm based on back propagation optimized by the beetle antennae search method (BAS-BPNN) is introduced to mathematically describe the random rotation of the cross-section. The elementary row-to-column transformation of the unit length RLCG parameter matrix is used to deal with the random transposition of the core. The discontinuity between segments generated by transposition is solved by introducing transition probability parameters. Finally, combined with the finite-difference time-domain (FDTD) algorithm, the crosstalk of the random cable bundle is obtained. The numerical experimental results show that the new method can reduce a lot of experimental work in the crosstalk problem of random cable bundle, and has higher accuracy and a wider frequency range.

INDEX TERMS Crosstalk, random cable bundle, beetle antennae search (BAS) algorithm, back propagation neural network (BPNN) algorithm, finite-difference time-domain (FDTD), multi-conductor transmission lines (MTLs).

I. INTRODUCTION

Hand-assembled random cable bundles are widely used for electrical interconnection between complex systems (such as in the aerospace and automotive machinery fields). The different wires are randomly gathered and fixed together by hand bundling. As the operating frequency increases and the types of cable bundles increase, the effects of crosstalk between these cable bundles cannot be ignored [1], [2].

The simpler uniform transmission line model can directly solve its transmission line equation to get crosstalk [3]. The model of the random cable bundle is uncertain, so the position of each cable core is random, and crosstalk cannot be solved by traditional methods.

Regarding the establishment of a random cable bundle model. In [4], Monte Carlo (MC) algorithm was introduced to divide the cable bundle into uniform sections with the same cross-section. The positions of the cable cores are randomly interchanged between the segments to statistically represent the random behavior of the manually assembled cable bundle. The random midpoint displacement (RMD) algorithm is another method [5], [6]. This method also divides the bundle into uniform cascade segments, but describes the position of the conductor along the bundle with fractal curves. The random displacement spline interpolation (RDSI) method is used to model a random cable bundle, and the model is used to predict the crosstalk of the cable bundle and evaluate

The associate editor coordinating the review of this manuscript and approving it for publication was Bo Pu.

the effectiveness of the method in an experimental environment [7]. Due to the characteristics of the algorithm, the constructed cable will cause unnatural discontinuities between adjacent beam segments.

Crosstalk of random cable bundle can be predicted using the cascade method [8], [9]. The traditional method is to solve the crosstalk by the chain parameter matrix method [10], [11]. But the accuracy of this method is not high, and the number of segments is related to the constructed cable bundle model. In [12]–[14], the FDTD algorithm is used to solve the time-domain and frequency-domain crosstalk of non-uniform cable bundles. The FDTD algorithm in Implicit-Wendroff format is unconditionally stable. Compared with the traditional FDTD algorithm, it can greatly reduce the crosstalk solution time.

This paper proposes to equivalent the transposition between cable cores to the elementary row-column transformation of the RLCG parameter matrix. It introduces transition probability parameters between different cross-sections to resolve discontinuities between adjacent segments, which greatly simplifies analysis of the influence of random transposition of cores on cable bundle crosstalk. The above references only considered the random interchange of the positions of the cores of the cable harness in a small segment. In fact, after the cores were interchanged, there was still a rotation factor in the cross-section relative to the ground. This paper introduces the BAS-BPNN algorithm to deal with the effects of rotation factors on the cable bundle [15], [16]. This algorithm has a strong nonlinear mapping ability [17], [18]. The transposition and rotation characteristics jointly determine the model of the random cable bundle and the RLCG parameter matrix of the cross-section. The obtained RLCG parameter matrix combined with the FDTD algorithm to obtain the crosstalk.

This paper is outlined as follows. In Section II, a model of random cable bundle is established. In Section III, First, the influence of cross-section rotation on the RLCG parameter matrix was analyzed using the BAS-BPNN algorithm. Then, the elementary transformation of the matrix was used to describe the effect of the random transposition of the cable core on the parameter matrix. Finally, the FDTD algorithm with Implicit-Wendroff difference scheme is used to solve the crosstalk. In Section IV, the new method proposed in this paper to analyze a specific random cable bundle model and compare it with simulation results. This paper is concluded in Section V.

II. MODELING OF RANDOM CABLE BUNDLE

The "randomness" of random cable bundle has its own characteristics. As shown in Fig.1, according to the idea of the cascade method, the n-core random cable bundle is divided into uniform small sections along the axial direction to assume the following characteristics:

(1) Each transmission line can be considered as a parallel transmission line.

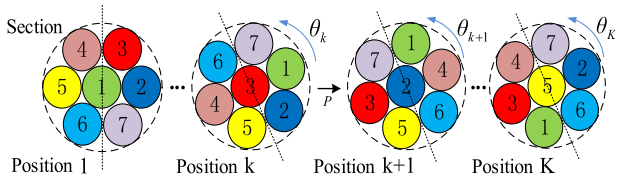

FIGURE 1. Cross-section model of the random cable bundle.

(2) The geometric shape of the cross-section can be considered as a circular outline, so the overall geometric shape of the cable bundle has a cylindrical outline.

(3) The structure and material of each cable core are the same.

To facilitate the description of the modeling process, a 7-core random cable bundle is used as an example. As shown in Fig.1, random changes occur along the axial center of a random cable bundle, which is characterized by cross-section rotation and cable core transposition.

Cross-section rotation means that there is a rotation angle θ_k for each small section of the cable. Since the direction of the cross-section rotation is arbitrary (assuming that the counter-clockwise rotation direction is positive direction), the range of the rotation angle can be taken as $\theta_k \in [-\theta_{\max}, \theta_{\max}]$. Where $\theta_{\max}$ is a parameter related to the length Δz of each segment and the diameter D of the cable core, which meets the experience formula:

$$\theta_{\max} = \begin{cases} \dfrac{4\Delta z}{\alpha n D} 180^\circ & \Delta z \le \dfrac{\alpha n D}{4} \\ 180^\circ & \Delta z > \dfrac{\alpha n D}{4} \end{cases} \tag{1}$$

where n is the number of cores in the cable bundle, and α is a correction constant, which usually takes a value of 1∼2, which indicates the correction value of the cable axis length when the cable bundle is twisted.

In addition to rotation, there is also a transposition between the core of cable bundle, which can be described by satisfying a uniformly distributed pseudo-random number. Introduce the probability transfer matrix $\mathbf{P}$ to approximate the actual core transposition situation and solve the problem of discontinuity of the conductor between segments.

$$\mathbf{P} = \begin{bmatrix} p_{11} & p_{12} & \cdots & p_{17} \\ p_{21} & p_{22} & \cdots & p_{27} \\ \vdots & \vdots & \ddots & \vdots \\ p_{71} & p_{71} & \cdots & p_{77} \end{bmatrix} \tag{2}$$

where p_{ij} represents the probability that the numbered i core and the numbered j core are transposed.

Although the effect of the cross-section after a certain angle of rotation can be the same as that produced by the transposition, but rotation alone does not allow the centerline beam (numbered 1 in Fig.1) to participate in transposition. To simulate the "randomness" of a random cable bundle, it is necessary to rotate the angle based on the core wire transposition.

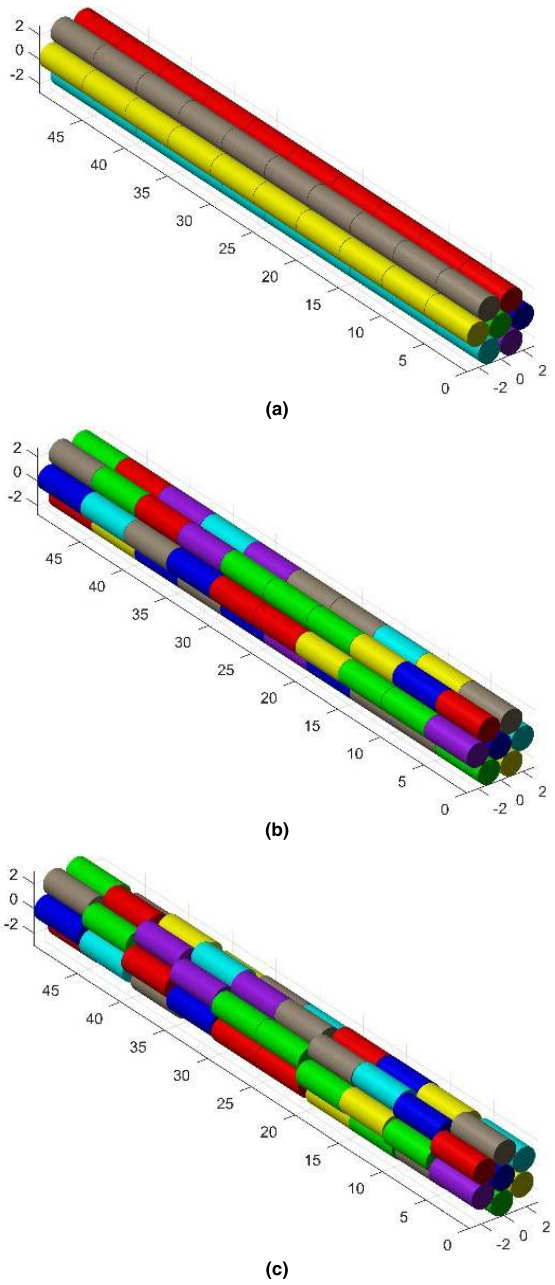

FIGURE 2. Random cable bundle model (a) Parallel cable model (b) Cable model after considering transposition (c) Cable model after considering rotation.

Fig.2 show a process for the establishment of a random cable bundle model divided into 10 segments, which satisfies the previously assumed conditions. Fig.2(a) is a model of a parallel cable bundle. The model after only considering the random transposition of the cable cores is shown in Fig.2(b). The geometry of the cross-section of each segment is constant relative to the reference ground. Without considering the rotation angle, if only two core wires are exchanged for each transposition, the cross-section between the front and back can be obtained by n-1 exchanges at most. Fig.2(c) is based on the model in Fig.2(b), considering the rotation factor, to obtain the final random cable bundle model.

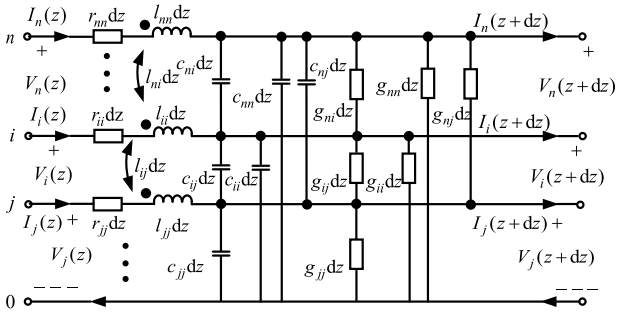

FIGURE 3. The per unit length equivalent circuit for MTLs.

III. ACQUISITION OF UNIT LENGTH PARAMETER MATRIX AND PREDICTION OF CROSSTALK

For the convenience of research, consider evenly divided transmission lines, each of which can be considered as parallel transmission lines. The circuit model under its unit length is shown in Fig.3.

The relationship of the transmission lines voltages and currents can be determined as follows [3]:

$$\frac{\partial \mathbf{V}(z,t)}{\partial z} + \mathbf{R}(z)\mathbf{I}(z,t) + \mathbf{L}(z)\frac{\partial \mathbf{I}(z,t)}{\partial t} = 0 \tag{3}$$

$$\frac{\partial \mathbf{I}(z,t)}{\partial z} + \mathbf{G}(z)\mathbf{V}(z,t) + \mathbf{C}(z)\frac{\partial \mathbf{V}(z,t)}{\partial t} = 0 \tag{4}$$

where $\mathbf{V}$(z,t) and $\mathbf{I}$(z,t) are the voltage and current vectors at different positions and different times on the transmission lines, both of which are n-dimensional. The $\mathbf{R}$(z), $\mathbf{L}$(z), $\mathbf{C}$(z) and $\mathbf{G}$(z) parameter matrices are variables related to the position z of the transmission lines, and they are all $n \times n$ order matrices.

A. CONSIDER THE RLCG PARAMETER MATRIX UNDER THE CONDITION OF SECTION CONDUCTOR ROTATION

Because the cable bundle is a random cable bundle, the rotation angle of the cross-section is also random. Different rotation angles correspond to different parameter matrices. It is difficult to obtain parameter matrices with arbitrary angles in the traditional way. Any determined rotation angle of the cross-section has its own corresponding parameter matrix, and there is a non-linear relationship between the rotation angle and the parameter matrix.

Therefore, this paper introduces a back propagation neural network algorithm optimized by the beetle antennae search method (BAS-BPNN) with strong nonlinear mapping ability. Because there are many elements in the parameter matrix of the random cable bundle, as the output of BPNN, the output of the network may fall into a local minimum [19], [20]. Therefore, the beetle antennae search method (BAS) was introduced to optimize the weight of BPNN. Network topology is shown in Fig.4.

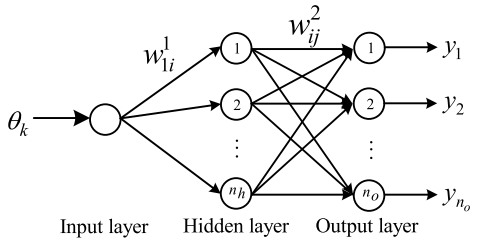

FIGURE 4. Topological structure of BAS-BPNN.

The input of the network is the rotation angle θ_k of the cross-section k, which belongs to the range (1). The output is the RLCG parameter matrix value of cross-section k. Because the RLCG parameters are symmetric matrices, the output can be represented by the vector $\mathbf{Y}$ as:

$$\mathbf{Y} = \left[\overline{\mathbf{R}}, \overline{\mathbf{L}}, \overline{\mathbf{C}}, \overline{\mathbf{G}}\right] = \left[\mathrm{y}_1, \mathrm{y}_2, \cdots, y_{n_o}\right] \tag{5}$$

where $\overline{\mathbf{R}}, \overline{\mathbf{L}}, \overline{\mathbf{C}}, \overline{\mathbf{G}}$ represents a row vector of triangular elements arranged on a parameter matrix.

The number of output layers n_o is determined by the RLCG parameter matrix. The number of hidden layers n_h is an empirical value determined by the number of input layers and output layers, which can be as follows:

$$n_h = 0.5\,(n_o + 1) + a, \quad a = 1, 2, \cdots 10 \tag{6}$$

The hidden layer uses the sigmoid function $f(\mathrm{x})$, and the output layer uses the linear function $g(\mathrm{x})$. They are as follows:

$$f\,(x) = \frac{1}{1 + e^{-x}} \tag{7}$$

$$g\,(x) = x \tag{8}$$

The weights w_{1i}^1 and w_{ij}^2 are optimized using the BAS optimization algorithm. The specific steps are as follows:

Step 1: Establish the optimized objective function. The output of the network is:

$$y_j = \sum_{i=1}^{n_h} \frac{w_{ij}^2}{1 + e^{-w_{1i}^1 \theta_k}} \tag{9}$$

For N sets of data, the mean square error between the network output value and the actual value is:

$$E(w_{1i}^1, w_{ij}^2) = \frac{1}{2N} \sum_{i=1}^{N} \sum_{j=1}^{n_o} \left(y_j - y_j'\right)^2 \tag{10}$$

where y_j' is the actual data of the given RLCG parameter matrix, and $E(w_{1i}^1, w_{ij}^2)$ is the optimized objective function.

Step 2: Initialize the position vector of beetle. The ownership value is listed as a single row vector $\boldsymbol{w}$, which represents the position of the beetle in the high-dimensional data space.

$$\boldsymbol{w}^{(0)} = rands\,(t, 1) \tag{11}$$

where t represents the dimension of the weight vector, and *rands* represents the generation of a t-dimensional row vector that obeys a uniform distribution.

Step 3: Calculate the left and right whisker positions and feeling intensity. The positions of the left and right whisker are as follows:

$$\begin{cases} \boldsymbol{w}_{\boldsymbol{R}}^{(n)} = \boldsymbol{w}^{(n-1)} + \dfrac{d}{2} \cdot \boldsymbol{dir}^{(n)} \\ \boldsymbol{w}_{\boldsymbol{L}}^{(n)} = \boldsymbol{w}^{(n-1)} - \dfrac{d}{2} \cdot \boldsymbol{dir}^{(n)} \end{cases} \tag{12}$$

where $w_{\boldsymbol{R}}$ and $w_{\boldsymbol{L}}$ represent the right and left whisker position of the beetle. d is the distance between the left and right whisker. $\boldsymbol{dir}^{(n)}$ represents the unit normal vector of the left whisker pointing to the right whisker, each time it is a randomly generated vector. n represents the n-th iteration calculation.

The left and right feeling intensity under the objective function (10) is:

$$\begin{cases} E_R^{(n)} = \dfrac{1}{2N} \displaystyle\sum_{i=1}^{N} \sum_{j=1}^{n_o} \left(y_j\left(\boldsymbol{w}_{\boldsymbol{R}}^{(n)}\right) - y_j'\right)^2 \\ E_L^{(n)} = \dfrac{1}{2N} \displaystyle\sum_{i=1}^{N} \sum_{j=1}^{n_o} \left(y_j\left(\boldsymbol{w}_{\boldsymbol{L}}^{(n)}\right) - y_j'\right)^2 \end{cases} \tag{13}$$

where $y_j\left(\boldsymbol{w}_{\boldsymbol{R}}^{(n)}\right)$ represents the network output value when the weight vector is $\boldsymbol{w}_{\boldsymbol{R}}^{(n)}$.

Step 4: Update the position of beetle.

$$\boldsymbol{w}^{(n+1)} = \boldsymbol{w}^{(n)} - \delta \cdot \boldsymbol{dir}^{(n)} \cdot sign\left(E_L^{(n)} - E_R^{(n)}\right) \tag{14}$$

where δ is the step size of the beetle, which is generally taken as $\delta = \sqrt{t}$. *sign* is a sign function.

Step 5: Convergence judgment. When the error between a set of output values of the neural network and a given value reaches a given target error ε, the next set of data training is performed. After the training of all data, find the average error E, if it reaches a given error η, proceed to the next iteration. If it does not satisfy the given error, the previous steps are processed until it reaches the maximum number of iterations, thereby obtaining the global minimum of the average error.

Through the BAS-BPNN algorithm, the RLCG parameter matrix at any rotation angle of the cross-section can be obtained, but the parameter matrix at this time is only the result considering the rotation factor.

B. CONSIDER THE RLCG PARAMETER MATRIX UNDER THE CONDITION OF SECTION CONDUCTOR TRANSPOSITION

The analysis in the previous summary only considers the rotation of the cross-section, and does not consider the transposition factor of the cable core. According to the previous random cable bundle model, it can be seen that the cores of the cable bundle in different sections have transposition changes. The transmission lines at different positions of the random cable bundle may have different parameter matrices, and the elements in the parameter matrices correspond to the row and column transformations.

The row and column transformations of the four parameter matrices are the same. For simplicity, the parameter matrix

can be expressed as:

$$\mathbf{M}=\begin{bmatrix} m_{11} & \cdots & m_{1i} & \cdots & m_{1j} & \cdots & m_{1n} \\ \vdots & \ddots & \vdots & \vdots & \vdots & \vdots & \vdots \\ m_{i1} & \cdots & m_{ii} & \cdots & m_{ij} & \cdots & m_{in} \\ \vdots & \vdots & \vdots & \ddots & \vdots & \vdots & \vdots \\ m_{j1} & \cdots & m_{ji} & \cdots & m_{ij} & \cdots & m_{jn} \\ \vdots & \vdots & \vdots & \vdots & \vdots & \ddots & \vdots \\ m_{n1} & \cdots & m_{ni} & \cdots & m_{nj} & \cdots & m_{nn} \end{bmatrix} \tag{15}$$

where $\mathbf{M}$ represents $\mathbf{R}$, $\mathbf{L}$, $\mathbf{C}$, and $\mathbf{G}$ parameter matrices of the initial cross-section, and $\mathbf{M}$ is a symmetric matrix. m_{ij} represents the specific resistance r_{ij}, inductance l_{ij}, capacitance c_{ij} and conductance g_{ij} corresponding to different parameter matrices.

After transposing the i-th wire and the j-th wire in Fig.3, the parameter matrix can be expressed as:

$$\mathbf{M}_k=\begin{bmatrix} m_{11} & \cdots & m_{1j} & \cdots & m_{1i} & \cdots & m_{1n} \\ \vdots & \ddots & \vdots & \vdots & \vdots & \vdots & \vdots \\ m_{j1} & \cdots & m_{jj} & \cdots & m_{ji} & \cdots & m_{jn} \\ \vdots & \vdots & \vdots & \ddots & \vdots & \vdots & \vdots \\ m_{i1} & \cdots & m_{ij} & \cdots & m_{ii} & \cdots & m_{in} \\ \vdots & \vdots & \vdots & \vdots & \vdots & \ddots & \vdots \\ m_{n1} & \cdots & m_{nj} & \cdots & m_{ni} & \cdots & m_{nn} \end{bmatrix} \tag{16}$$

The relationship between $\mathbf{M}$ and $\mathbf{M}_k$ can be expressed as:

$$\mathbf{M}_k=\mathbf{T}_{ij}\mathbf{M}\mathbf{T}_{ij} \tag{17}$$

$\mathbf{T}_{ij}$ is the elementary transformation matrix, which can be written as:

$$\mathbf{T}_{ij}=\begin{bmatrix} 1 & 0 & \cdots & 0 & \cdots & 0 & \cdots & 0 \\ 0 & 1 & \cdots & 0 & \cdots & 0 & \cdots & 0 \\ \vdots & \ddots & \ddots & \vdots & \vdots & \vdots & \vdots & \\ 0 & 0 & \cdots & 0 & \cdots & 1 & \cdots & 0 \\ \vdots & \vdots & \vdots & \vdots & \ddots & \vdots & \vdots & \vdots \\ 0 & 0 & \cdots & 1 & \cdots & 0 & \cdots & 0 \\ \vdots & \vdots & \vdots & \vdots & \vdots & \vdots & \ddots & \vdots \\ 0 & 0 & \cdots & 0 & \cdots & 0 & \cdots & 1 \end{bmatrix} \tag{18}$$

The parameter matrix of the cross section at any position k in Fig.2(b) can be obtained by the elementary transformation of n-1 times. The specific parameter matrix is as follows:

$$\mathbf{M}_k=\mathbf{T}_{ij}^{n-1}\cdots\mathbf{T}_{ij}^{1}\mathbf{M}\mathbf{T}_{ij}^{1}\cdots\mathbf{T}_{ij}^{n-1} \tag{19}$$

where $\mathbf{T}_{ij}^{m}$ represents the m-th elementary row and column transformation of the parameter matrix, $m=1,2,\cdots,n-1$. i and j represent the i-th, j-th rows (columns) of the matrix, $i,j=1,2,\cdots,n$. $i(j)$ is not the same in all exchanges.

Considering that with the increase of the number of segments, the wires in the front and back cross-sections will not be randomly displaced in actual situations, and they need to meet the continuity requirements of the wires. Therefore, the constraint of a certain probability transition matrix $\mathbf{P}$ is satisfied. As shown in cross-section 1 in Fig.1, when the length of the segment is small, the probability of transposition between the core wire 2 and core wire 5 in the back section is very low.

All probabilities of transposition of each cross-section core meet the following requirements:

$$\sum_{m=1}^{n-1}p_{ij}^{m}\geq p_{\min} \tag{20}$$

where p_{ij}^{m} represents the probability value satisfied by the i and j core transposition, and p_{min} represents the minimum probability value required by all the core transposition.

$$\mathbf{R}=\begin{bmatrix} 1.56 & 0.285 & 0.314 & 0.337 & 0.296 & 0.245 & 0.237 \\ 0.285 & 1.42 & 0.297 & 0.142 & 0.076 & 0.079 & 0.203 \\ 0.314 & 0.297 & 1.541 & 0.348 & 0.148 & 0.082 & 0.109 \\ 0.337 & 0.142 & 0.348 & 1.555 & 0.299 & 0.11 & 0.077 \\ 0.296 & 0.076 & 0.148 & 0.299 & 1.426 & 0.207 & 0.078 \\ 0.245 & 0.079 & 0.082 & 0.11 & 0.207 & 1.306 & 0.148 \\ 0.237 & 0.203 & 0.109 & 0.077 & 0.078 & 0.148 & 1.297 \end{bmatrix} \tag{21}$$

$$\mathbf{L}=\begin{bmatrix} 495.37 & 206.32 & 243.69 & 243.68 & 206.33 & 139.23 & 139.18 \\ 206.32 & 512.03 & 248.39 & 165.74 & 115.28 & 79.376 & 143.34 \\ 243.69 & 248.39 & 593.28 & 287.21 & 165.74 & 89.495 & 104.88 \\ 243.68 & 165.74 & 287.21 & 593.2 & 248.38 & 104.89 & 89.468 \\ 206.33 & 115.28 & 165.74 & 248.38 & 512.15 & 143.37 & 79.354 \\ 139.23 & 79.376 & 89.495 & 104.89 & 143.37 & 356.39 & 88.61 \\ 139.18 & 143.34 & 104.88 & 89.468 & 79.354 & 88.61 & 356.24 \end{bmatrix} \tag{22}$$

If the probability of a core transposition does not satisfy formula (20), a uniformly distributed random number is re-generated to encode the core, and the probability value is recalculated until formula (20) is satisfied. The unit length RLCG parameter matrix at any segment in Fig.2(b) can be obtained by (19) and (20).

C. PREDICTION OF CROSSTALK

The previous chapters considered the influence of the random cable bundle cross-section rotation and core transposition on the parameter matrix.

In section A, the RLCG parameter matrix of the initial cross-section and the output parameters of the BAS-BPNN algorithm can be extracted by ANSYS simulation software based on the finite element method (FEM). On this basis, consider the effect of core rotation. The elementary transformation matrix mentioned in section B is used to perform row and column transformation on the RLCG parameter matrix obtained in section A, so as to achieve the ''random characteristic'' of transposition and rotation in a random cable bundle.

The crosstalk solution will be combined with the FDTD method, which uses the Implicit-Wendroff difference format [21]. The transmission line equations (3) and (4) are differentiated to obtain a discretized transmission line equation. The difference method is an unconditionally stable difference method. The time step and the space step are not limited by the stability conditions, and it has a great advantage in the calculation efficiency of crosstalk.

The random cable bundle is evenly divided into multiple segments, and the RLCG parameter matrix of each segment can be obtained by the proposed method. Use the discretized transmission line equation to get the final crosstalk. The process of obtaining crosstalk is shown in Fig.5.

IV. NUMERICAL EXPERIMENT VERIFICATION AND ANALYSIS

In order to verify the correctness of the proposed method, a 7-core random cable bundle is used as an example to verify the proposed method. The conductors in the cable bundle are all copper conductors with a diameter of 0.8 mm. The material of the insulating layer is polyvinyl chloride (PVC), which has a thickness of 0.6 mm and a relative dielectric constant of 2.7. The length of the random cable bundle is 1 m along the axial direction. Both ends of the wire are connected to a 50Ω resistor, and some related parameters are shown in Table.1.

The initial reference cross-section model is shown in Fig.6. and its angle θ_1 is a fixed value. The RLCG parameter matrix was extracted using ANSYS software. The RLCG parameter matrix of the initial reference cross-section is (21) and (22), as shown at the bottom of the previous page, (23) and (24), as shown at the bottom of the next page. The units are Ω/m, nH/m, pF/m, and mS/m.

The model in Fig.6 is an axisymmetric figure with respect to the ground. The angle of rotation only needs to consider $0 \sim 60°$ relative to the reference section. The rest of the

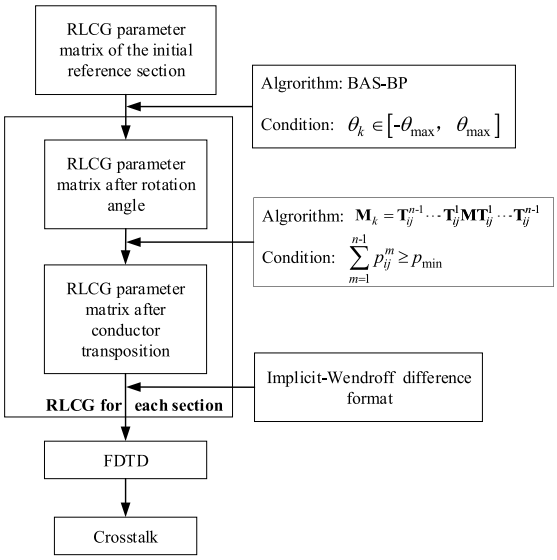

FIGURE 5. Process of random cable bundle crosstalk prediction.

TABLE 1. Basic parameters.

Name	Parameter
wire diameter	0.8mm
insulation layer thickness	0.6mm
insulation material	PVC (2.7)
cable bundle length	1m
height of center wire from ground	3mm
correction constant	1.5
hidden layers of neural network	15
BAS iterations	100

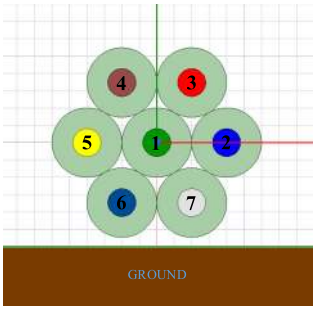

FIGURE 6. Initial reference cross-section.

range can be obtained by row and column transformation. The RLCG matrix values are sampled every 3°, and a total of 20 groups are used as training data for BAS-BPNN. The total computation time of the training process in Fig.7 is 487.41s. The error in equation (10) is only 0.3%. The average error of 8 randomly selected test sets is shown in Figure 8, and the results are all below 0.3%.

Random cable bundles were simulated in CST Cable Studio software based on the transmission line matrix (TLM) method [22]. Its arrangement in CST is shown in Fig.9.

Near-end crosstalk (NEXT) and far-end crosstalk (FEXT) of each line are defined as follows:

$$NEXT_n = 20\log_{10}\frac{V_{n,NEXT}}{V_S} \tag{25}$$

$$FEXT_n = 20\log_{10}\frac{V_{n,FEXT}}{V_S} \tag{26}$$

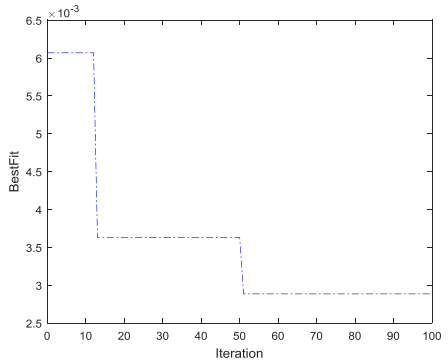

FIGURE 7. Iterative process of BAS-BPNN.

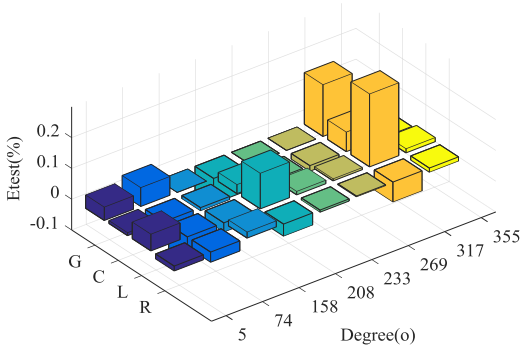

FIGURE 8. Average error histogram of test set.

where V_S represents the applied interference voltage on line 1, $V_{n,NEXT}$ represents the disturbed voltage of the n-th line near the interference voltage terminal, and $V_{n,FEXT}$ represents the disturbed voltage of the n-th line away from the interference voltage terminal. $n = 2, \cdots, 7$.

The predicted values of crosstalk of random cable bundles with 100 and 500 segments are shown in Fig.10 and Fig.11, respectively. The solid green line is the result of the new method, with a total of 42 curves in 6 groups. The calculation time for each group of curves is 0.51 hour and 2.69 hour. The red dotted line is the envelope value of the result obtained by the method in this paper. The envelope value indicates the

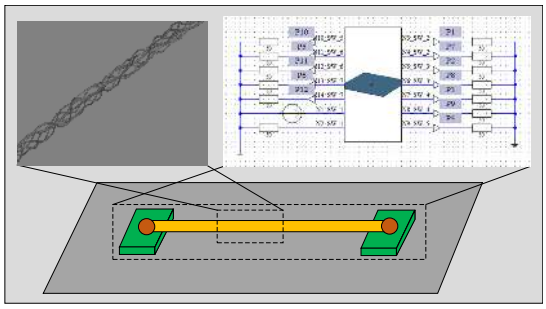

FIGURE 9. Simulation of a seven-core random cable bundle in CST.

"worst case" crosstalk of the cables. The black dotted line is the envelope value only in the BPNN method. The magenta dotted line uses the Monte Carlo (MC) method to consider the crosstalk envelope value under the condition of only random transposition. The solid blue line is the result of a CST (TLM) simulation of a fixed model drawn randomly.

It can be seen from Fig.10 and Fig.11 that the CST results of the randomly selected model are within the upper and lower envelope values of the proposed method, indicating the correctness of the new method. This can save a lot of crosstalk calculation time and improve prediction accuracy. The consistency of results in the lower frequency band ($f <$ 100MHz) are slightly better than the higher frequency band ($f >$ 100MHz). As the number of segments increases, the more stringent the constraints that each cross section meets, the tighter the twists in its cable bundle will be. So this will make the corresponding crosstalk more concentrated, and the upper and lower envelope values in the result will be closer. Therefore, in the high frequency range ($f >$ 100MHz), the crosstalk under 500 segments is more concentrated than under 100 segments.

It can be seen from Fig.10 and Fig.11 that the upper and lower envelope values of the proposed method are narrower than those of the BPNN and MC methods in the low frequency band ($f <$ 100MHz). Although the CST results are also in the upper and lower envelope values of other

$$\mathbf{C} = \begin{bmatrix} 91.308 & -15.156 & -15.144 & -15.156 & -15.149 & -14.881 & -14.881 \\ -15.156 & 65.12 & -20.643 & -1.021 & -0.188 & -0.506 & -18.462 \\ -15.144 & -20.643 & 63.592 & -21.068 & -1.02 & -0.122 & -0.665 \\ -15.156 & -1.021 & -21.068 & 63.618 & -20.65 & -0.664 & -0.122 \\ -15.149 & -0.188 & -1.02 & -20.65 & 65.108 & -18.454 & -0.506 \\ -14.881 & -0.506 & -0.122 & -0.664 & -18.454 & 80.822 & -15.107 \\ -14.881 & -18.462 & -0.665 & -0.122 & -0.506 & -15.107 & 80.827 \end{bmatrix} \tag{23}$$

$$\mathbf{G} = \begin{bmatrix} 0.351 & -0.059 & -0.058 & -0.058 & -0.059 & -0.058 & -0.058 \\ -0.059 & 0.208 & -0.072 & -0.002 & -0.0002 & -0.0014 & -0.07 \\ -0.058 & -0.072 & 0.207 & -0.073 & -0.0016 & -0.0002 & -0.0015 \\ -0.058 & -0.002 & -0.073 & 0.207 & -0.072 & -0.0015 & -0.0002 \\ -0.059 & -0.0002 & -0.0016 & -0.072 & 0.209 & -0.07 & -0.0015 \\ -0.058 & -0.0014 & -0.0002 & -0.0015 & -0.07 & 0.249 & -0.064 \\ -0.058 & -0.07 & -0.0015 & -0.0002 & -0.0015 & -0.064 & 0.249 \end{bmatrix} \tag{24}$$

TABLE 2. The average width of the envelope value (dB) under 100 segments.

Frequency	0~100MHz		100~500MHz		500~1000MHz	
Type	NEXT	FEXT	NEXT	FEXT	NEXT	FEXT
BAS-BPNN	4.527	2.026	21.180	9.026	24.293	20.726
BPNN	6.641	3.712	24.522	10.839	27.175	25.108
MC	10.924	5.319	23.078	13.478	27.346	27.032

TABLE 3. The average width of the envelope value (dB) under 500 segments.

Frequency	0~100MHz		100~500MHz		500~1000MHz	
Type	NEXT	FEXT	NEXT	FEXT	NEXT	FEXT
BAS-BPNN	2.730	1.117	15.246	4.292	22.369	14.476
BPNN	4.285	2.433	16.214	5.016	24.390	17.928
MC	4.331	2.584	14.191	5.021	22.391	13.791

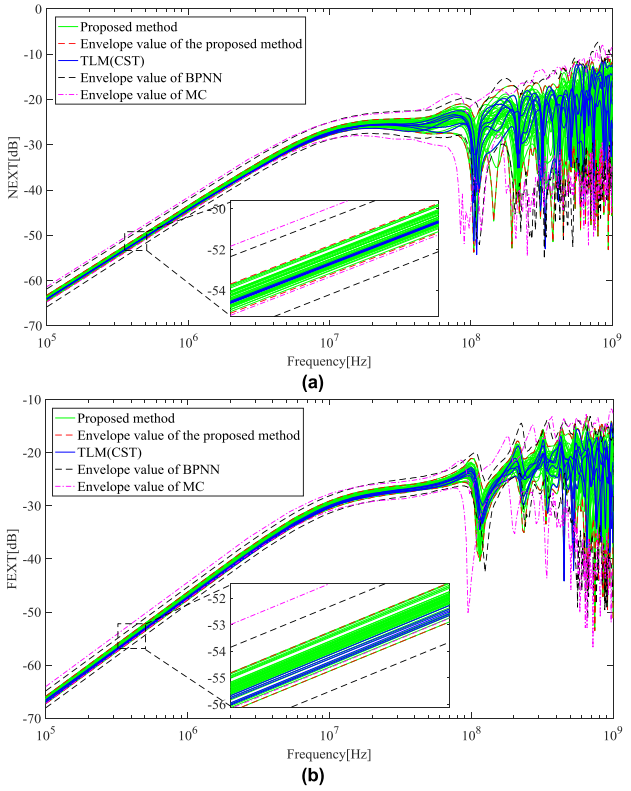

FIGURE 10. Predicted and simulated values under 100 segments (a) near-end crosstalk (NEXT) (b) far-end crosstalk (FEXT).

methods, the new method is more accurate than other methods. Table.2 and Table.3 show the average envelope widths of NEXT and FEXT in different frequency ranges. It can be seen from the table that the average width of the envelope value of the proposed method is also smaller than that of the BPNN and MC methods in the high frequency range (f > 100MHz). The largest difference between the average envelope widths is 6.397dB.

In addition to the width of the envelope value, the BPNN method (MC method) has a corresponding offset at the resonant frequency (f > 100MHz) compared to the CST. But the

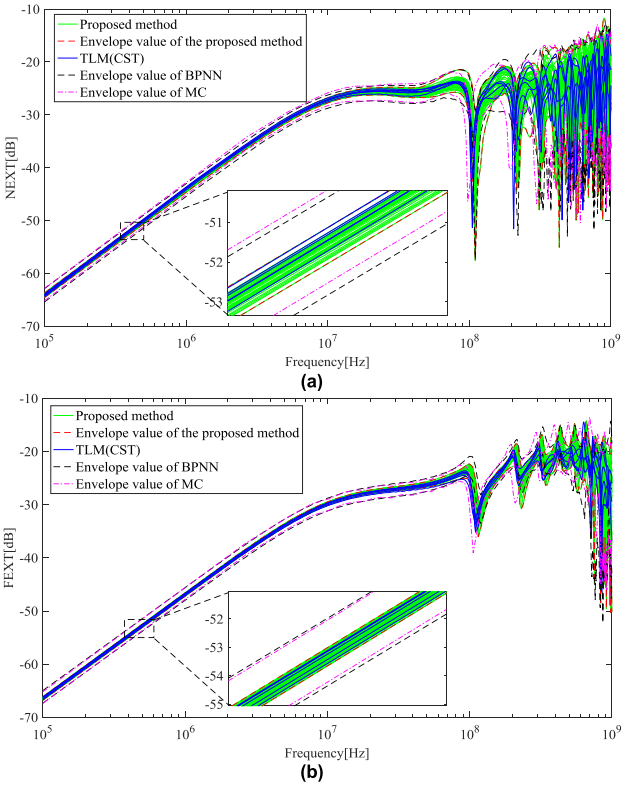

FIGURE 11. Predicted and simulated values under 500 segments (a) near-end crosstalk (NEXT) (b) far-end crosstalk (FEXT).

resonance point of the proposed method is in good agreement with the CST. It can be seen that at a few high frequencies, the lower envelopes solved by the new method are not completely consistent with the CST. It may be because the number of iterations of the crosstalk solution is too small, which causes the transposition and rotation changes to not be reflected well.

V. CONCLUSION

This paper studies the crosstalk of random cable bundle based on the ideas of the transmission line cascade method and the FDTD method. First, the BAS-BPNN algorithm is used to solve the characteristics of rotation in a random cable bundle, and the maximum rotation angle affected by the number of segments is considered to simulate the actual rotation. Secondly, the transposition is considered on the basis of rotation. The elementary row-to-column transformation of the matrix is used to handle the transposition of the cable core and the transition probability parameter is introduced to resolve the discontinuity caused by the transposition between segments. Finally, the crosstalk is solved by using the FDTD method.

The comparison and verification of numerical experiments show that the BAS-BPNN algorithm can accurately describe the RLCG parameter matrix affected by the cross-section rotation, and the results of the BAS-BPNN are better than the BPNN algorithm. Compared with the previous method, the new method proposed in this paper has better prediction ability and range. The crosstalk distribution is relatively

concentrated in the low frequency band, and the high frequency band is relatively diffuse. It will be more difficult to accurately predict its range.

REFERENCES

[1] S. Chabane, P. Besnier, and M. Klingler, "A modified enhanced transmission line theory applied to multiconductor transmission lines," *IEEE Trans. Electromagn. Compat.*, vol. 59, no. 2, pp. 518–528, Apr. 2017.
[2] Y. Wang, Y. S. Cao, D. Liu, R. W. Kautz, N. Altunyurt, and J. Fan, "A generalized multiple-scattering method for modeling a cable harness with ground connections to a nearby metal surface," *IEEE Trans. Electromagn. Compat.*, vol. 61, no. 1, pp. 261–270, Feb. 2019.
[3] C. R. Paul, *Analysis of Multiconductor Transmission Lines*, 1st ed. Hoboken, NJ, USA: Wiley, 1994.
[4] S. Shiran, B. Reiser, and H. Cory, "A probabilistic method for the evaluation of coupling between transmission lines," *IEEE Trans. Electromagn. Compat.*, vol. 35, no. 3, pp. 387–393, Aug. 1993.
[5] S. Salio, F. Canavero, J. Lefebvre, and W. Tabbara, "Statistical description of signal propagation on random bundles of wires," in *Proc. 13th Int. Zurich Symp. Electromagn. Compat.*, Zurich, Switzerland, 1999, p. 8.
[6] D. Weiner and G. Capraro, "A statistical approach to EMI—Theory and experiment Part II," in *Proc. IEEE Int. Symp. Electromagn. Compat.*, Atlanta, GA, USA, Aug. 1987, pp. 448–452.
[7] S. Sun, G. Liu, J. L. Drewniak, and D. J. Pommerenke, "Hand-assembled cable bundle modeling for crosstalk and common-mode radiation prediction," *IEEE Trans. Electromagn. Compat.*, vol. 49, no. 3, pp. 708–718, Aug. 2007.
[8] S. Salio, F. Canavero, D. Lecointe, and W. Tabbara, "Crosstalk prediction on wire bundles by Kriging approach," in *Proc. IEEE Int. Symp. Electromagn. Compatibility. Symp. Rec.*, Washington, DC, USA, Nov. 2000, pp. 197–202.
[9] S. A. Pignari, G. Spadacini, and F. Grassi, "Modeling field-to-wire coupling in random bundles of wires," *IEEE Electromagn. Compat. Mag.*, vol. 6, no. 3, pp. 85–90, Nov. 2017.
[10] G. Spadacini, F. Grassi, and S. A. Pignari, "Field-to-wire coupling model for the common mode in random bundles of twisted-wire pairs," *IEEE Trans. Electromagn. Compat.*, vol. 57, no. 5, pp. 1246–1254, Oct. 2015.
[11] Y. Sun, J. Wang, W. Song, and R. Xue, "Frequency domain analysis of lossy and non-uniform twisted wire pair," *IEEE Access*, vol. 7, pp. 52640–52649, 2019.
[12] A. Tatematsu, F. Rachidi, and M. Rubinstein, "A technique for calculating voltages induced on twisted-wire pairs using the FDTD method," *IEEE Trans. Electromagn. Compat.*, vol. 59, no. 1, pp. 301–304, Feb. 2017.
[13] V. R. Kumar, B. K. Kaushik, and A. Patnaik, "An accurate FDTD model for crosstalk analysis of CMOS-gate-driven coupled RLC interconnects," *IEEE Trans. Electromagn. Compat.*, vol. 56, no. 5, pp. 1185–1193, Oct. 2014.
[14] P. Zhang, X. Du, J. Zou, J. Yuan, and S. Huang, "Iterative solution of MTL based on the spatial decomposition and the second-order FDTD," *IEEE Trans. Magn.*, vol. 54, no. 3, Mar. 2018, Art. no. 7200404.
[15] T. Rashid, *Make Your Own Neural Network*, 1st ed. Charleston, SC, USA: CreateSpace Independent Publishing Platform, 2016.
[16] X. Y. Jiang and S. Li, "Beetle antennae search without parameter tuning (BAS-WPT) for multi-objective optimization," Cornell Univ., Ithaca, NY, USA, Nov. 2017. [Online]. Available: https://arxiv.org/abs/1711.02395
[17] B. Cannas, A. Fanni, and F. Maradei, "A neural network approach to predict the crosstalk in non-uniform multiconductor transmission lines," in *Proc. IEEE Int. Symp. Circuits Syst.*, Phoenix-Scottsdale, AZ, USA, Jun. 2002, pp. 573–576.
[18] F. Dai, G. Bao, and D. Su, "Crosstalk prediction in non-uniform cable bundles based on neural network," in *Proc. 9th Int. Symp. Antennas, Propag. EM Theory*, Guangzhou, China, Nov. 2010, pp. 1043–1046.
[19] X. Yi, "Selection of initial weights and thresholds based on the genetic algorithm with the optimized back-propagation neural network," in *Proc. 12th Int. Conf. Fuzzy Syst. Knowl. Discovery (FSKD)*, Zhangjiajie, China, Aug. 2015, pp. 173–177.
[20] Q. Wu, Z. Ma, G. Xu, S. Li, and D. Chen, "A novel neural network classifier using beetle antennae search algorithm for pattern classification," *IEEE Access*, vol. 7, pp. 64686–64696, 2019.
[21] L. Brancik and B. Sevcik, "Fully time-domain simulation of multiconductor transmission line systems: Implicit wendroff and euler methods within modified nodal analysis," in *Proc. Joint INDS ISTET*, Klagenfurt, Austria, Jul. 2011, pp. 1–6, doi: 10.1109/inds.2011.6024812.
[22] W. L. Yu, Z. W. Yan, and J. Cao, "Simulation analysis of crosstalk and radiation effects of cables inside aerocraft," in *Proc. IEEE Int. Symp. Antennas*, Xian, China, 2012, pp. 755–758, doi: 10.1109/ISAPE.2012.6408881.

CHAO HUANG was born in Anhui, China. He received the B.S. degree from the School of Electrical Engineering and Automation, Anhui University of Technology, Ma'anshan, China, in 2018. He is currently pursuing the master's degree in electrical engineering with Nanjing Normal University, Nanjing, China. His main research interests include multiconductor transmission lines and EMC.

YANG ZHAO received the B.E., M.E., and Ph.D. degrees in power electronic technology from the Nanjing University of Aeronautics and Astronautics, Nanjing, China, in 1989, 1992, and 1995, respectively. He is currently a Professor with Nanjing Normal University. His research interests include electromagnetic compatibility, power electronics, and automotive electronics.

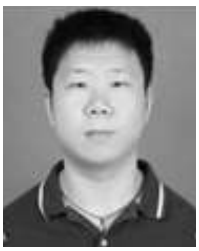

WEI YAN received the M.S. degree in electrical engineering and the Ph.D. degree in physics and electronics from Nanjing Normal University, in 2014 and 2011, respectively. He is currently a Doctor and an Associate Professor with Nanjing Normal University. He is a Senior Member of the China Electrical Technology Association and an Evaluation Expert of the Electromagnetic Compatibility Calibration Specification of China.

QIANGQIANG LIU was born in Anhui, China. He received the B.S. degree from the School of Electrical Engineering and Automation, Anhui University of Science and Technology, Huainan, China, in 2018. He is currently pursuing the master's degree in electrical engineering with Nanjing Normal University, Nanjing, China. His major research interest includes the new technology of electrical engineering.

JIANMING ZHOU was born in Jiangsu, China. He received the B.S. degree from the School of Electrical Engineering and Automation, Tianping College, Suzhou University of Science and Technology, Suzhou, China, in 2019. He is currently pursuing the master's degree in electrical engineering with Nanjing Normal University, Nanjing, China. His major research interest includes the new technology of electrical engineering.